Petrology and Geochemistry of the Granitoids and Their Deformed-Metamorphic-Metasomatic Variants in the Kasturigattu – Gudarukoppu area, near SE Margin of the Cuddapah Basin, Andhra Pradesh, India and Their Bearing on the U-mineralisation in the Area

Ch. Sudhakar[1] and R. Dhana Raju[2]

[1]502, Shanti Imperial, Santosh Nagar Colony, Mehdipatnam, Hyderabad – 500 028, [2]1-10-284/1, Begumpet, Brahmanawadi Lane 5, Hyderabad – 500 016,
Corresponding author: R. Dhana Raju

Abstract: The Kasturigattu (K) – Gudarukoppu (G) area (i) is intensely sheared, (ii) forms a part of the Crystalline Complex (CC) close to the SE margin of the Cuddapah Basin (CB) in Andhra Pradesh, India, and (iii) lies in between the sedimentary rocks of the Nallamalai Group of the Mesoproterozoic CB to its west and the schistose rocks of the Archaean Nellore Schist Belt (NSB) to its east. Petrography-wise, CC consists of (a) basement biotite granitoid; (b) schists (with major mineralogy of quartz, feldspars, biotite, chlorite, epidote, sericite and sphene); and (c) gradational, deformed-metamorphic-metasomatic variants of (a) and (b), comprising schistose/gneissose granite and cataclasite/mylonite/phyllonite, besides (d) intrusive basic rocks of epidiorite, metadolerite and orthoamphibolite . Of these, quartz-feldspar-biotite schist around Kasturigattu and quartz-apatite cataclasite/mylonite and apatite(secondary)-bearing quartzofeldspathic schist near Gudarukoppu are radioactive, assaying 0.01-0.31% U_3O_8 and are characterised by alterations of biotitisation and chloritisation (in both the K and G areas), apatitisation (in the G area) and sericitisation (in the K area), attesting to K-Fe-Mg-P metasomatism in the K-G area. Mineragraphic study on the radioactive samples had shown that the U-mineralisation in the area is manifested as uraninite, coffinite, pitchblende and uranophane (the last as fracture-fillings and surface encrustations), associated with sulphides (more in the K-area) of pyrite, chalcopyrite, pyrrhotite, galena (Pb being radiogenic) and minor molybdenite and arsenopyrite, and oxides of rutile and martitised magnetite. Geochemically, (i) the granitoid is peraluminous (with normative corundum > 3% and A/CNK > 1.1), sodic with $Na_2O/K_2O > 1$, depleted in Rb and Sr (each down to 114 ppm) and relatively enriched in Ba (up to 1295 ppm) and U (up to 42 ppm) with Th/U < 1;(ii) the deformed-metamorphic-metasomatic variants, namely cataclasite and mylonite, and schists exhibit two patterns - silicification with enrichment of SiO_2 up to 86 wt. % and strong depletion in most of other major and minor oxides as well as most trace elements; and de-silicification or basification, marked by strong depletion in SiO_2 and notable enrichment in FeO^t, MgO, CaO, K_2O, P_2O_5 and LOI as well as trace elements of V, Cr, Co, Ni, Cu, Ga, Sr, Y and REE, with potential U-mineralisation associated more with the latter. The U-mineralisation in the K-area is of 2 types – (i) high-temperature, syn-magmatic, older type in the form of euhedral to subhedral uraninite (pre-sulphides) and (ii) low-temperature, younger, hydro (epi)-thermal type, manifested as coffinite and pitchblende (post-sulphides), with the latter, dominant over the former, and almost exclusively in the G-area. The controls for U-mineralisation in the K-G area are: structural (shear zone); petrological (fertile granitoid, and mineralised schists and deformed-metamorphic-metasomatic variants, i.e., cataclasite, and mylonite; geochemical (de-silicified zones preferred); metamorphic (greenschist to epidote amphibolite facies); metasomatic (K-Fe-Mg-P metasomatism);and mineralogical alterations, viz., dominant biotitisation, lesser sericitisation, chloritisation and dominant apatitisation (in the G-area).
Keywords: Petrology, geochemistry, granitoids and their variants, U-mineralisation, Kasturigattu – Gudarukoppu area, Andhra Pradesh, India.

I. Introduction

The Mesoproterozoic Cuddapah Basin (CB), including the Neoproterozoic Kurnool basin within it, is the second largest (~ 44,000 sq km area) intracratonic *Purana* basin in India (Nagaraja Rao *et al.*, 1987) and is well known for its diverse and vast mineral resources - both metallic and non-metallic - of base metals (Cu, Pb and Zn), iron, manganese, limestone, dolomite, barite, asbestos, phosphorite, dimensional stones and diamonds, all of which are being exploited since long [Geological Survey of India (GSI), 1975; Kurien, 1980; Dutt, 1986;

Nagaraja Rao *et al.*, 1987]. Until mid-1980s, CB was considered as a 'Thorium Province' due to location of many Th-occurrences by the geo-scientists of the Atomic Minerals Directorate for Exploration and Research (AMD) of the Department of Atomic Energy (DAE), Govt. of India working from early1950s in it, which afterwards became potential for 'Uranium', starting with the discovery of the U-mineralisation in its Vempalle Dolomite and Pulivendla conglomerate/quartzite by GSI (Sundaram *et al.*, 1987). Sustained exploration for U by numerous AMD geo-scientists since 1986 has changed CB from an earlier considered Th-province to 'India's emerging U-hub' (Dhana Raju, 2009) due to establishment of notable U-deposits/-prospects, both within and in the SW and SE environs of CB. Thus, exploration during the last 8 decades led to the establishment of India's total U-resources of 3,00,034 te *in situ* U_3O_8 (2,54,429 t U) (as on May, 2018; un-starred question no. 1316 of Lok Sabha, to be answered on 25-07-2018; www.amd.gov.in of AMD) by AMD, under different categories of resources. Of these, ~ 60% is contributed by the large tonnage, but low-grade (~ 0.045% U_3O_8) stratabound phosphatic, siliceous carbonate-hosted U-deposit (presently under exploitation by the UCIL of DAE) in the Tummalapalle – Giddankipalle area in SW part of CB (Vasudeava Rao *et al.,* 1988; Dhana Raju *et al.*, 1993; Jeyagopal and Dhana Raju 1998). In addition to this vast, rare type U-deposit, other U-deposits/prospects both within and in the SW- and SE-environs of CB are as follows: the unconformity-proximal type U-deposit, mostly in the basement granite and lesser in its overlying quartzite, in the Lambapur - Peddagattu - Chitrial - Koppunuru areas in N and NE parts of CB (Sinha *et al.,* 1995; Jeyagopal *et al.,*1996) and U-prospects of (i) hydrothermal-type mineralisation in the quartzite in the Gandi area in SW part (Umamaheswar *et al.* 2001), (ii) fracture-controlled mineralisation around Lakkireddipalle in the southern environs (Bidwai and Madhusudan Rao, 1988; Dhana Raju *et al.,* 2002; Dhana Raju *et al.*, 2018) and (iii) shear zone-hosted mineralisation close to the SE-margin in the Kasturigattu – Gudarukoppu - Kulluru area (Thimmiah *et al.,* 1986; Veerabhaskar *et al.,* 1991; Rai *et al.,* 1995; Dhana Raju *et al.,* 2002; Dhana Raju *et al.*, 2018a and b) (Fig. 1a). In the present paper, petrology (both petrography and mineragraphy) and geochemistry (of whole-rocks) of the granitoids and their deformed-metamorphic-metasomatic variants, *viz.,* cataclasites and mylonites, and schists in the Kasturigattu (K) – Gudarukoppu (G) area, together with related brief accounts of geological setting, methods adopted and materials used, metamorphism – metasomatism and controls of U-mineralisation are presented, and their bearing on the U-mineralisation in the K-G area (Sudhakar, 1996) are discussed.

II. Geological Setting

The K - G area forms a part of the crystalline complex along the SE environs of CB (Fig. 1b). The area is bound by the thrust-contact to its west with the Nallamalai Group of folded sequence of the Cuddapah Supergroup and by the Nellore Schist Belt (NSB) to its east. Regionally, the area is composed of metavolcanic rocks and migmatites, followed by Quartz-Pebble Conglomerate (QPC) and quartzite. To the west of the Kasturigattu hill, the predominant range of the Nallamalai quartzite occurs. The schists and granitoids, which underly metasedimentary rocks, constitute the early Proterozoic basement rocks that are exposed immediately to the SE margin of CB. Amongst the schists, the main rock types are feldspathised biotite schist, quartz-chlorite schist, quartz-sericite-sphene-chlorite schist, sphene-epidote-biotite-quartz schist and phyllite, while the granitoids comprise biotite granitoid, granite mylonite and schistose granite mylonite. Basic rocks, represented by amphibolites, meta-dolerite and epidorite, and belonging to the Kandra volcanic suite (within NSB), occur intruding both the schists and granitoids. Younger intrusive granitoid was emplaced in these older rocks. Unconformably overlying the schists and gneisses are QPC, quartzite and phyllite. Unconformably overlying the basement are the Bairenkonda quartzites of the Nallamalai Group of the Cuddapah Supergroup, with a polymictic conglomerate at the base, representing the Eparchaean Unconformity. The entire succession of the basement crystalline rocks, with a veneer of the overlying Bairenkonda quartzite, thrust over the Nallamalai Group of sediments all along the E-margin of CB. Tectonically, the area represents the interface between the Archaean Dharwar craton and Proterozoic Eastern Ghats mobile belt, and is marked by a prominent regional thrust with associated shear zone running nearly 300 km parallel to the craton-margin. There are younger (Neoproterozoic) plutons of Kanigiri, Podili, etc., close to this margin, with the A-type Kanigiri granite enriched in Nb, Y, REE, U and Th (Banerjee *et al.*, 1983; Thirupathi *et al.,* 1996). According to Leelanandam (1990), the Kandra volcanic suite of basic rocks occurring close to the area under study could possibly represent an ophiolite (?). Structurally, the K-G area is very close to the thrust contact of the basement crystalline rocks over the Nallamalai sedimentary formation of CB. Two major shears, trending N-S and NW-SE occur in this area, with trends of joint system being NW-SE, NE-SW, N-S and E-W. Dip of the shear planes are sub-vertical due west. Quartz veins intruded the basement. At places, drag folds are present in the eastern part of the shear zone. Overall, the area shows doubly plunging isoclinal fold systems and the radioactive shear zone passes through one of the axial plane of the anticline (Rai *et al.,* 1992).
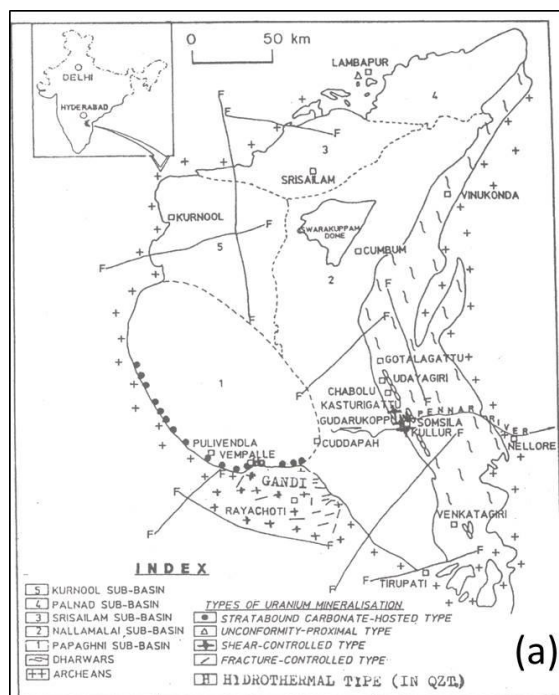
Fig. 1a. Cuddapah basin and its sub-basins, with loca-
tion of different types of U-deposits and -prospects,
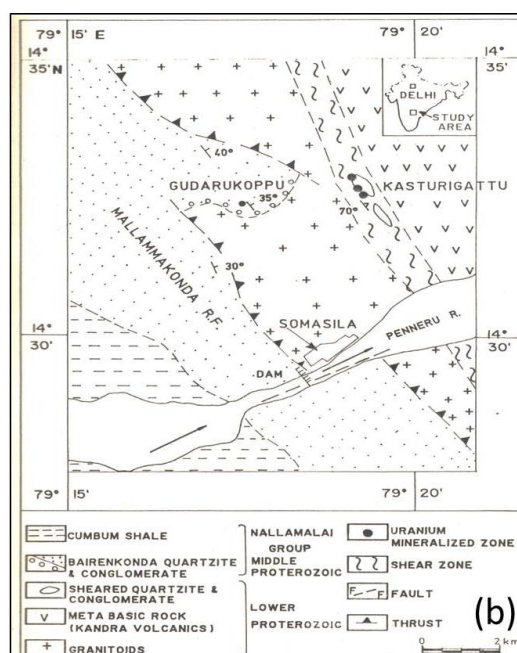both within and in its SW and SE environs

Fig. 1b. Geological map of the Kasturigattu – Guda-
rukoppu area, Nellore district, Andhra Pradesh,
India (Source: Veera Bhaskar *et al.*, 1991).

III. Methods and Materials

Different methods of investigation adopted in the present study (i.e.) collection of samples in the field, preparation of specimens and thin- and polished thin-sections for both transmitted and reflected light microscopic study, Solid State Nuclear Track Detector (SSNTD) study, using alpha-sensitive Cellulose Nitrate (CN)-85 film on both radioactive hand specimens and polished thin sections to locate radioactive minerals, chromogram study on both radioactive hand specimens and polished thin sections to locate leachable U-minerals, fluorescence study of samples under Ultra Violet (UV) light study on selected radioactive samples, to know colour and intensity of fluorescence of uranyl minerals like uranophane, X-Ray Diffraction (XRD) study for confirmation of primary (identified by reflected light microscopy) and secondary U-minerals (indicated by fluorescence study under UV light), preparation of sample powders of -200 # for radiometric analysis of U and Th by γ-ray spectrometry and -300 # for chemical analysis of whole-rocks by various instrumental methods, titrimetry and gravimetry for different major, minor and trace (including RE) elements, as per the methods detailed by Satyanarayana (1986) and Dhana Raju (2009a), as well as the materials used in each of the above are given elsewhere (Dhana Raju *et al.,*2018b); for more details, the reader is referred to Dhana Raju (2009b and c). As a check on the chemical analysis, International Rock Standards – AGV-1 and BCR-2 – were analyzed. The per cent error, with respect to values of the standards, was found to be < 1 for SiO_2, Al_2O_3, Fe_2O_3 and CaO; < 3 for TiO_2, FeO, MgO, MnO, Na_2O and K_2O; and mostly < 10 to rarely < 15 for the rest of the elements, including trace elements.

IV. Petrology

In the Kasturigattu (K) – Gudarukoppu (G) area, the rock types met with in the outcrops and drill core are mainly of 3 types, *viz.,* granitoids and their deformed variants like cataclasites and mylonites; schists; and intrusive basic rocks; petrology of these rocks under the sub-heads of petrography and mineragraphy (only of radioactive samples), studied from the K and G areas are given below, separately.

Kasturigattu (K) area: Four rock types (i.e.) granitoids, mylonites, schists and basic intrusive rocks were studied from this area and the petrography of these are given in the following, along with mineragraphy of radioactive samples.

Petrography

(a) *Granitoids:* The granitoids of this area were subjected to intense shearing resulting in the formation of their deformed variants like granite mylonite and schistose granite mylonite. These rocks are leucocratic and medium to coarse grained with hypidiomorphic granular texture. Mineralogy-wise, they have major minerals of quartz, orthoclase, sodic plagioclase and biotite, with microcline instead of orthoclase in the granitoids from Malla-mmakonda. Both feldspars are altered to sericite, more so the plagioclase. Biotite defines the schistose texture. Sericite, sphene, epidote and muscovite constitute the minor minerals, with accessory apatite, zircon and zoisite. Sphene is found altering to some opaque mineral. Epidote, biotite and muscovite occur mostly along fractures, along

which recrystallised quartz occurs. These rocks have undergone deformation, evidenced by bending of lamellae in and fragmentation of plagioclase.

(b) *Mylonites*: *Granite mylonite* is a dark coloured rock with mylonitic texture and fragmented quartz and feldspar, embedded in a biotite-rich dark mass that shows crude foliation. Quartz, orthoclase, sericitised plagioclase and biotite are the major minerals. Biotite is mostly brownish green in colour and mainly found elongated. At places, clusters of fine quartz are found as a result of recrystallisation. Epidote and muscovite are the minor minerals, with zircon, sphene, zoisite, apatite, monazite and opaque ore minerals being accessories. Zoisite and muscovite occur mainly along fractures, whereas zircon and monazite as inclusions in biotite. Deformational effects are manifested by fragmentation and reduction in grain size of original coarse grained quartz and feldspar. Relict coarse grains are embedded in the fine-grained matrix. *Schistose granite mylonite* is a dark coloured, hard and indurated rock, with a crude foliation around porphyroblasts of altered and sheared plagioclase and quartz, embedded within a mass of pulverised quartzofeldspathic material, abundant granular apatite, biotite, chlorite and clusters of sphene, with green tourmaline being abundant in a few samples. Biotite rims around feldspars in some samples and occupies spaces in between the fragments in some other samples, pointing out that biotitisation is a late process.

(c) *Schists*: These include quartz-biotite schist, quartzofeldspathic schist, chlorite-epidote-quartz-biotite schist, sphene-epidote-biotite-sericite schist and quartz-chlorite schist. These rocks consist of chlorite (pleochroic from pale to dark green), biotite, epidote, sericite and quartz as major minerals, sphene and apatite as minor, and zircon and opaque ore minerals as accessories. Sericite is the alteration product of plagioclase. Biotite is brownish green in colour and contains inclusions of epidote, sphene, apatite and zircon, with pleochroic haloes around sphene. Quartz occurs mainly as veins and interstitial grains. At places, recrystallised quartz occurs as fine-grained clusters. Quartzofeldspathic schist is dark greenish grey coloured and very fine grained. It consists mainly of pulverised and recrystallised quartz and plagioclase, with lesser amounts of biotite, apatite, grass-green tourmaline, epidote and sphene. Plagioclase occurs as both porphyroblasts and fine grains, with deformational effects in the form of shearing and dislocation of twin lamellae.

(d) *Intrusive Basic* Rocks: These include epidiorite, meta-dolerite and orthoamphibolite. *Amphibolite* is dark, hard, indurated and medium- to fined-grained rock consisting of hornblende, actinolite, epidote, sphene, altered plagioclase and recrystallised quartz as the major minerals, with minor biotite and chlorite, and accessory opaque ore minerals. Some samples show interlocking texture. The observed mineral assemblage, absence of diopside and relict igneous texture suggest it as an orthoamphibolite, derived from a parental gabbro/basalt under regional metamorphism. *Epidiorite* is a dark coloured, fine-grained and massive rock, with biotite, chlorite, epidote-zoisite, sphene, hornblende and quartz as major minerals, with minor plagioclase and calcite. Biotite shows stain-haloes around zoisite due to leaching of its iron. Chalcopyrite and pyrrhotite are the common opaque minerals. *Meta-dolerite* is a dark coloured, hard, fine-grained and indurated rock. It exhibits interlocking texture, defined by plagioclase, hornblende, orthopyroxene and ilmenite, varying to metamorphic planar texture, marked by association of granular hornblende, pyroxene, biotite, fine quartz, plagioclase and ilmenite. A few phenocrysts of plagioclase are embedded in fine groundmass of plagioclase, quartz, hornblende and sometimes biotite that is an alteration product of hornblende.

Mineragraphy

Radiometric survey in the Kasturigattu area has shown promising radioactivity due to uranium in the quartzofeldspathic biotite schist, with radiometric values ranging from 0.01 to 0.19% U_3O_8, with negligible Th.

Source, nature and phases of U-mineralisation: The main sources of radioactivity are uraninite and pitchblende, which, under the SSNYD study, registered dense alpha tracks on the CN-85 film. Sparse alpha tracks are registered from anatase and leucoxene. Other radioactive minerals identified are coffinite, brannerite and urano-thorite. *Uraninite* occurs usually as euhedral crystals (Fig. 2a) with pitted surface and alteration along its boundary. It occurs as *inclusions* in feldspar and quartz, and is replaced by sulphides (Fig. 2b). It contains tiny inclusions of high reflective galena, with its lead being radiogenic. Uraninite is usually rimmed by a reddish brown border due to radioactive bombardment. Radiation cracks, emerging from the uraninite and extending into the host minerals of feldspar and quartz, are recorded. *Coffinite* (Fig. 2c) occurs as clusters of idiomorphic crystals and looks like gangue (in oil) with low reflectivity. It contains a number of tiny inclusions of pyrite and pyrrhotite, and is associated with carbonaceous matter and anatase. It is usually found enclosed by a thin rim of chlorite. *Pitchblende* occurs as tiny vein-lets and ultrafine disseminations. Besides, minor radioactivity is contributed by zircon, allanite and U-associated with biotite. Amongst the other ore minerals, associated with the above radioactive phases, sulphides are abundant and include pyrite, chalcopyrite, pyrrhotite, galena (with radiogenic Pb) and minor arsenopyrite, with occasional presence of molybdenite. In a few samples, pyrrhotite is the most dominant ore mineral, followed by chalcopyrite and pyrite. These sulphides are associated with epidote and altered sphene. Most of the pyrite occurs as tiny inclusions in epidote. Tiny inclusions of pyrite and chalcopyrite are noted in fine-grained sericite and coarser biotite. Pyrrhotite is also found as small inclusions in major rock-forming and radioactive minerals, besides as discrete coarse grains. Intergrowth of pyrrhotite with pyrite and chalcopyrite is recorded, at places. These sulphide minerals also occur as vein- and fracture-fillings.

Gudarukoppu (G) area: In this area, migmatites, cataclasites/mylonites and schists occur. Their petrography and mineragraphy of radioactive samples are given in the following.

Petrography
(a) *Migmatites*: These rocks are medium to coarse grained and dark coloured, with impersistent bands and, at places, small augens of light coloured minerals. They exhibit gneissocity, due to preferred orientation of platy minerals, quartz and feldspars. Plagioclase, orthoclase, quartz, biotite and muscovite are the major minerals, with accessory minerals of epidote, sphene, apatite and zircon. Primary quartz is dominant over the recrystallised (secondary) quartz. These rocks underwent intense deformation, evidenced by step-like deformation of twin lamellae of plagioclase and bending and kinking of micas, with broken zircon, at places.

(b) *Cataclasites/Mylonites*: *Biotite granite cataclasite* is a dark coloured, medium to coarse grained rock with cataclastic texture and consists of plagioclase (~ 50 vol. %), quartz (~ 20%) and biotite (~ 20%; with pleochroic haloes) and microcline perthite (~ 5%) as major minerals, with accessory zoisite, apatite, sphene and zircon. Fine grained quartz and biotite are interstitial and swerve around coarser clasts of feldspar. The rock exhibits deformational effects of both ductile (bending of cleavage and kinking in biotite and twin lamellae of plagio-clase) and brittle (fragmentation of quartz and feldspars). *Ferruginous quartz-apatite cataclasite* is a fine-grained, yellowish brown coloured and weathered *radioactive* rock, with yellow coloured fracture-fillings and surface encrustations of fluorescent (in bright yellow green colour under UV light) *uranophane* (U^{6+}-mineral, identified by XRD). The rock consists mainly of apatite (~ 70 vol. %) with subordinate amount of quartz and ferruginous material. Apatite is present in 2 modes – one of coarse grained, rounded to sub-rounded type (0.18-0.66 mm; Fig. 2d) and the other of fine-grained (< 0.09 mm) type that occurs as in-fillings along the grain boundaries of the former. Granular quartz is intimately associated with the fine-grained apatite. The rock is highly fractured, with an irregular network of veins filled by limonite, smectite, U-minerals and, at places, chlorite (antigorite) and biotite. Irregular patches of goethite, associated with hematite, exhibit colloform banding. Fine granular anatase occurs as fillings along grain-boundary. Minute specks of pyrite are noted.

(c) *Schists/phyllites*: *Quartzofeldspathic biotite schist* is a dark coloured, schistose *radioactive* rock, with abundant biotite and fractured porphyroclasts of orthoclase and plagioclase, set in a groundmass of biotite, sericite and quartz, having different degrees of recrystallisation. Biotite and sericite define the schistosity and swerve around the porphyroclasts. Zoned zircon is the accessory mineral. More or less same mineralogy occurs in the phyllites, with major difference being phyllitic texture instead of schistosity of schists.

Mineragraphy
Radioactivity of the order of 0.36% U_3O_8 and 0.05% ThO_2 was recorded in the quartzofeldspathic biotite schist.

Source, nature and phases of U-mineralisation: Four types of sources of radioactivity occur in this area:
(i) Major contribution (~ 70%) of radioactivity is from yellowish coloured secondary U-mineral, *uranophane* (identified by XRD study) present as fracture-fillings in surface samples (Fig. 2e).
(ii) Subordinate amount of radioactivity is due to *pitchblende* (Fig. 2f), occurring as very thin stringers and vein-lets, in association with limonitic patches.
(iii) Adsorbed U within limonite, smectite and chlorite, as indicated by scattered alpha-tracks on CN-85 film. (iv) Sparse alpha-tracks are recorded on CN-85 film from a few grains of apatite, indicating it as a source of very low order radioactivity.

The above minerals are associated with sulphides of pyrite, pyrrotite, chalcopyrite and galena (Pb being radiogenic) and oxides of rutile and martitised magnetite; however, the sulphides and other ore minerals are much less in the Gudarukoppu area, as compared to that in the Kasturigattu area.
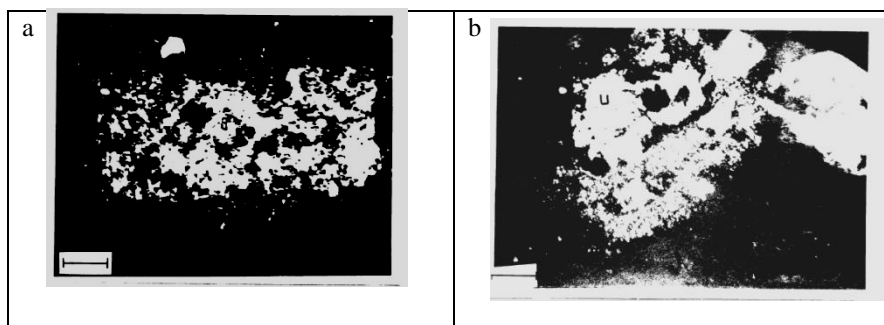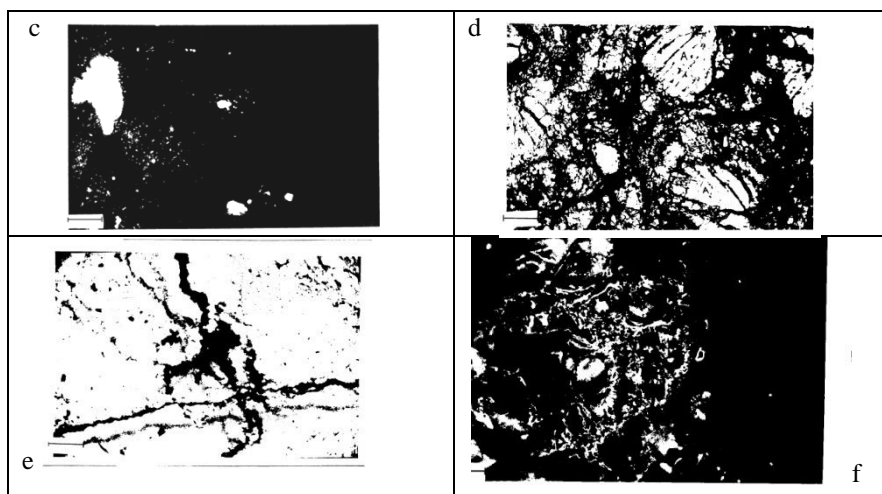
Fig. 2a. Euhedral *Uraninite* (U) with galena (g; Pb radiogenic) inside. Quartzofeldspathic schist.
Kasturigattu. Refl. Light. 1N oil; bar: 0.13 mm. (Source: Veera Bhaskar *et al.*, 1991).
Fig. 2b. *Uraninite* (U), replaced by sulphide (white, fine grains with higher reflectivity). Quartzofeldspathic
schist. Kasturigattu. Refl. Light. 1N oil; bar: 0.13 mm.
Fig. 2c. *Coffinite* (c, reflectivity merging almost with that of gangue minerals), associated with clusters of zircon
and tiny inclusions of sulphides (white, pyrite). Kasturigattu. Refl. Light. 1N oil; bar: 0.03 mm.
Fig. 2d. Subrounded aggregate of apatite (A), with granulation along margins. Note the granular apatite and
infiltration of fine quartz along the grain boundary. Irregular network of patches filled with limonite
and clay. Quartz-apatite cataclasite, Gudarukoppu. Tr. Light, 1N, Bar: 0.45 mm.
Fig. 2e. Cross-cutting fractures filled with secondary U-mineral (U, *uranophane*), with its corresponding alpha
tracks kept offset. Quartz-apatite cataclasite, Gudarukoppu. Tr. Light, 1N, Bar: 0.36 mm.
Fig. 2f. *Pitchblende* (P, as fine-grained network) along the grain boundaries of the gangue minerals and along
other weak planes, in association with limonite. Quartz-apatite cataclasite, Gudarukoppu. Tr. Light, 1N,
Bar: 0.04 mm.

V. Geochemistry

Major, minor (as oxides, in wt. %) and trace element (in ppm) chemical analysis of 18 whole-rock samples:
(a) 8 of granitoids [4 each from the Kasturigattu (K) and Gudarukoppu (G) areas] (Table 1); (b) schists (4
from the K-area) and quartz-apatite cataclasites, phyllites and schists (each 2 samples) from the G-area (10 samples in
Table 2), and Rare Earth Element [REE, in ppm; determined by the Instrumental Neutron Activation Analysis
(INAA)] analysis of 11 whole-rock samples, selected from the above 18 samples (Table 3; 6 samples from the K-area
and 5 from the G-area) are tabulated. The data in these 3 tables are examined in the following, area-wise, (i.e.)
Kasturigattu K) and Gudarukoppu (G), mainly to arrive at the (i) general *geochemical patterns*, rock type-wise, and
(ii) *inferences* drawn from these patterns for each analysed rock type.

Kasturigattu (K) area
Granitoids (Table 1): Major, minor and trace element geochemical patterns of these rocks are as follows:
1. The biotite granite from the Mallammakonda hill (sample no. M-15, Table 1) consists of high silica (72 wt.
%) and alumina (14%), more or less equal amounts of soda and potash, 1% CaO and low contents of FeO and MgO
and is, thus intermediate between low-Ca and high-Ca granites (*cf.* Turekian and Wedepohl, 1961).
2. This intermediate nature of this granite between low-Ca and high-Ca granite is also reflected by its trace
element contents of Rb, Ba and Sr. However, its Ni, Cr and Co contents are relatively more than that of even high-Ca
granite, whereas its Y and Zr contents are less than that of even low-Ca granite. Furthermore, it's Pb, Ga and Ce
(Table 3) contents are 2 or more orders than that of both average low-Ca and high-Ca granitoids.
3. This granite is marked by relatively higher content of Au (38 ppb) and low value of Zr/Hf value of 25, as
against more than 40 in normal granitic rocks.
4. This granite is strongly peraluminous, with A/CNK of 1.26.

Granite Mylonites (Table 1):
1. The granite mylonites (K-4, 23 and 26; Table 1), compared to the nearby Mallammakonda parental granite,
show two modes of major elemental changes. Thus, the granite mylonite sample, K-4, compared to the biotite granite
of Mallammakonda (M-15), is marked by depletion in SiO_2, K_2O and enrichment in Al_2O_3, Fe^t, MgO, TiO_2 and LOI,
whereas the other two samples of granite mylonite (K-23, 26) show the opposite patterns with enrichment in SiO_2 and
depletion in Al_2O_3, Fe^t, MgO, CaO, alkalies and LOI. These major elemental changes are designated, respectively, as
de-silification or *basification* and *silicification*.

Table1. Chemical analysis (major and minor oxides, in wt. %, and trace elements, in ppm) of the Granitoids and their deformed variants from the Kasturigattu (K) area (K-4, 9, 26, 23) area, Gudarukoppu (G) area (G-1, 10, 3) and Mallammakonda hill (M-15), near SE margin of the Cuddapah basin, Andhra Pradesh, India*

Sl. No.	K-4	K-9	K-26	K-23	G-1	G-10	G-3	M-15
SiO$_2$	66.36	78.88	85.52	84.65	69.80	49.30	67.20	72.14
Al$_2$O$_3$	15.56	11.23	7.86	8.90	15.60	15.90	16.50	14.07
Fe$_2$O$_3$	0.85	0.32	0.06	0.15	0.69	2.40	0.90	0.34
FeO	4.68	1.26	0.95	1.47	2.20	3.40	2.70	1.51
MgO	2.78	0.85	0.38	0.71	2.03	4.30	2.20	0.95
CaO	1.04	0.64	0.27	0.32	0.50	9.32	0.80	1.08
Na$_2$O	3.00	3.09	2.70	2.05	4.60	3.40	2.80	3.69
K$_2$O	2.87	1.59	0.60	1.15	2.30	4.60	2.80	3.69
TiO$_2$	0.65	0.13	0.06	0.23	0.50	0.38	< 0.01	0.22
P$_2$O$_5$	0.13	0.10	0.08	0.05	0.20	3.60	0.40	0.13
MnO	0.05	0.03	0.01	0.02	< 0.01	0.03	0.01	0.03
LOI	1.76	0.99	0.32	0.44	1.80	2.00	1.60	0.71
Total	**99.73**	**99.11**	**98.81**	**100.14**	**100.22**	**98.63**	**99.71**	**98.05**
V	57	13	9	11	112	147	89	74
Cr	85	34	20	27	26	262	25	29
Co	18	< 4	< 4	< 4	5	36	9	8
Ni	42	8	10	8	25	91	22	25
Cu	86	5	17	8	24	> 100	18	22
Ga	20	15	14	17	23	> 30	24	26
Rb	76	< 25	< 25	< 25	33	82	101	114
Sr	70	54	36	36	76	160	96	114
Y	63	< 10	< 10	< 10	28	232	25	< 10
Zr	156	251	304	310	105	324	73	99
Ba	1294	1218	330	552	390	672	86	910
Pb	30	30	90	20	14	113	15	51
U	42	25	237	18	8	378	17	< 10
Th	23	17	57	6	8	15	15	-
Au (ppb)	32	28	n.d.	n.d.	n.d.	n.d.	< 10	30
Sc	10.8	2	n.d.	n.d.	n.d.	n.d.	5.5	4.1
Cs	< 1	< 1	n.d.	n.d.	n.d.	n.d.	1.8	< 1
Ta	0.8	0.7	n.d.	n.d.	n.d.	n.d.	3.2	2.6
Hf	5.2	4.1	n,d.	n.d.	n.d.	n.d.	5.8	4.2

*From Sudhakar (1996). K-4: Biotite granite; K-9: Silicified granite; K-26: Silicified muscovite-biotite granite; K23- Granite mylonite; G-1: Migmatite; G-10: Biotite granite cataclasite; G-3: Biotite granite; and   M-15: parental, fertile 'Biotite granite'.   n.d.: not determined.
Analysts: Drs. DSR Murty and Anita Mary, Chemistry Lab., Southern Region, AMD, Bangalore.

2. Thus, compared to the biotite granite of Mallammakonda (M-15), the silica-depleted and Fe, Mg-enriched granite mylonite (K-4) is characterised by higher contents of Ni, Co, Cr, Sc, Hf and Ba, and depletion in Pb, whereas the silica-enriched ones (K-23, 26) show the opposite pattern of depletion in Ni, Co, Cr, V, Sc, Hf and Ba, and enrichment in Pb (one sample). However, both the silica-depleted and silica-enriched granite mylonites, compared to the parental biotite granite of Mallammakonda, show abnormal increase in the contents of U, Th and Zr, and notable depletion of Rb, Sr and Ce (Table 3), thereby attesting to their high mobility during mylonitisation.

3. The above contrast in the pattern of major elemental contents of the analysed rocks is also reflected in their trace element contents. Thus, compared to the biotite granite of Mallammakonda (M-15), the silica-depleted and Fe, Mg-enriched granite mylonite (K-4) is characterised by higher contents of Ni, Co, Cr, Sc, Hf and Ba, and depletion in Pb, whereas the silica-enriched ones (K-23, 26) show the opposite pattern of depletion in Ni, Co, Cr, V, Sc, Hf and Ba, and enrichment in Pb (one sample). However, both the silica-depleted and silica-enriched granite mylonites, compared to the parental biotite granite of Mallammakonda, show abnormal increase in the contents of U, Th and Zr, and notable depletion of Rb, Sr and Ce (Table 3), thereby attesting to their high mobility during mylonitisation.

4. Gold (Au) content in the mylonites, compared to the parental biotite granite, is low, but its content in silica-depleted and Fe-Mg-enriched mylonite is much higher than that in the silica-enriched and Fe-Mg depleted mylonites. This attests to a sympathetic variation of Au with Fe-Mg-enrichment.

5. The ∑ REE is more in the biotite granite, as compared to that of the granite mylonites, with much of   ∑ REE being accounted by LREE (Table 3). Although the ∑REE content of biotite granite, compared to that of the mylonites, is much more, the content of HREE in the biotite granite is less than that of the granite mylonites, particularly the silica-depleted one (K-4).

6. The chondrite-normalized REE-patterns (Fig. 3a) show an overall enrichment of LREE over HREE in both biotite granite and granite mylonites. However, the degree of this enrichment is much higher in the biotite granite and decreases notably in the granite mylonites, particularly in the silica-depleted granite mylonite (K-4), which is evidenced by sharp decrease in the value of (La/Lu)$_{cn}$ and (Ce/Yb)$_{cn}$ from 69 to 50 in biotite granite to 9 and 5-8 in the silica-depleted granite-mylonite.

7.　　In the Eu-anomaly also, there is a marked change from biotite granite to silica-depleted granite mylonite through silica-enriched granite mylonites, respectively, documented by negative Eu-anomaly to positive Eu-anomaly through almost no anomaly (Fig. 3a).

Table 2. Chemical analysis (major and minor oxides, in wt. %, and trace elements, in ppm) of the Schists (K-17, 20, 11 and 15) from the Kasturigattu (K) area and Phyllites　(G-7, 8), Schists (G-17, 11) and Quartz-Apatite (vein) Rock (G-2A, 2B) from Gudarukoppu (G) area, near the SE Margin of the Cuddapah basin, A.P., India*

Sl. No.	K-17	K-20	K-11	K-15	G-7	G-8	G-17	G-11	G-2A	G-2B
SiO_2	51.80	52.61	60.94	72.96	53.80	52.20	58.80	62.10	16.06	17.38
Al_2O_3	21.13	20.42	18.40	14.11	13.90	15.60	19.40	10.60	3.50	1.92
Fe_2O_3	2.42	0.90	0.56	0.23	2.10	3.20	2.60	0.14	1.90	1.58
FeO	3.47	7.18	2.52	0.50	8.20	5.90	3.80	7.40	0.40	0.36
MgO	1.36	4.38	1.76	0.32	9.23	7.77	1.30	3.10	1.05	1.15
CaO	4.20	1.27	2.94	2.15	0.90	0.99	0.09	8.10	42.00	41.80
Na_2O	0.51	2.20	6.38	4.50	0.50	0.30	0.90	1.80	0.70	0.14
K_2O	7.25	6.23	2.26	1.58	2.50	5.60	7.20	4.50	0.60	0.46
TiO_2	2.88	0.84	0.56	0.22	1.60	1.80	0.98	0.73	< 0.01	< 0.01
P_2O_5	0.73	0.58	1.25	0.25	0.40	0.40	0.30	0.50	31.60	31.34
MnO	0.05	0.07	0.05	0.03	0.04	0.04	0.02	0.11	0.02	0.02
LoI	3.82	2.95	1.77	1.95	5.70	5.45	3.40	1.60	1.80	1.20
Total	**99.64**	**99.63**	**99.39**	**98.80**	**98.87**	**99.25**	**98.79**	**100.68**	**99.63**	**97.36**
V	143	142	24	8	251	223	201	152	196	229
Cr	29	79	32	21	198	236	197	180	81	109
Co	19	18	6	< 4	97	59	62	29	34	34
Ni	31	25	9	<4	116	131	90	82	61	67
Cu	8	5	8	7	35	26	42	31	> 100	68
Ga	>30	29	21	17	> 30	> 30	> 30	27	16	18
Rb	175	204	53	15	93	170	186	236	30	n.d.
Sr	< 25	57	137	140	< 25	32	24	456	1336	n.d.
Y	48	43	24	22	84	70	44	45	>1000	> 1000
Zr	230	209	191	87	189	173	156	151	299	359
Ba	2330	3146	1452	1166	72	288	590	600	354	n.d.
Pb	30	19	65	96	20	49	47	13	> 200	> 200
U	58	7	153	110	4	85	4	3	1504	2595
Th	11	8	4	74	7	7	17	22	26	78
Au (ppb)	33	44	n.d.	n.d.	< 20	48	n.d.	n.d.	< 10	n.d.
Sc	60	15	n.d.	n.d.	34	27.5	n.d.	n.d.	13.2	n.d.
Cs	< 1	2	n.d.	n.d.	< 1	2	n.d.	n.d.	n.d.	n.d.
Ta	1.8	2.5	n.d.	n.d.	1	1.1	n.d.	n.d.	1.6	n.d.
Hf	7..0	6.5	n.d.	n.d.	4	5.2	n.d.	n.d.	n.d.	n.d.

*From Sudhakar (1996). n.d.: not determined. Analysts: Drs. DSR Murty and Anita Mary, Chemistry Lab., SR, AMD, Bangalore.

Table 3. Rare Earth Elements (REEs, in ppm) of the granitoids (K-4, 9, 23) and schists (K-17, 20) from the Kasturigattu (K) area, biotite granite from the Mallammakonda (M-15) and migmatite (G-1), biotite granite cataclasite (G-10), phyllites (G-7, 8) and quartz-apatite (vein) rock (G-2A) from the Gudarukoppu (G) area, near the SE margin of the Cuddapah basin, Andhra Pradesh, India*

REE	K-4	K-9	K-23	K-17	K-20	M-15	G-1	G-10	G-7	G-8	G-2A
La	27.0	8.0	28.0	18.0	37.0	103.0	19.0	27.0	88.0	33.0	725
Ce	36.0	12.0	49.0	32.0	60.0	185.0	32.0	39.0	125.0	53.0	1052
Nd	22.0	6.0	23.0	21.0	38.0	80.0	23.0	24.0	69.0	21.0	425
Sm	3.5	1.4	3.0	5.6	7.2	9.2	2.8	8.2	12.6	7.2	85
Eu	1.8	1.1	1.0	1.2	3.5	1.3	1.0	3.0	2.3	2.0	30
Tb	0.5	< 0.03	0.5	1.1	0.8	0.55	0.5	2.6	1.6	1.3	38
Tm	0.45	0.3	0.3	1.3	0.7	< 0.3	< 0.3	1.6	1.0	0.9	13.5
Yb	1.5	0.6	0.9	6.5	3.2	0.9	1.6	9.5	4.0	3.6	83
Lu	0.3	0.2	0.1	0.9	0.45	0.15	0.25	1.3	0.6	0.55	11.2

*From Sudhakar (1966). Sample index as in Tables 1 and 2. Analyst: N. Satyanarayana, INAA Lab., AMD Hq., Hyderabad.

From the above noted elemental patterns in the parental biotite granite of Mallammakonda and granite mylonites of the Kasturigattu-area, the following *inferences* are drawn.

1.　　The parental biotite granite, when subjected to mylonitisation has led to the formation of 2 types of mylonites, *viz*., silica-depleted, with Fe-Mg enrichment on one side (*de-silicification* or *basification*) and the other of silica-enriched, with Fe-Mg depletion (*silicification*).

2.　　During mylonitisation, there are notable changes in major, minor and trace elements. Thus, in the silica-depleted and Fe-Mg-enriched de-silicified mylonite, there is concomitant increase in the contents of Ni, Co, Cr, Ba, Sc

and Hf, whereas in the silica-enriched and Fe-Mg depleted silicified mylonite, there is marked depletion of Ni, Co, Cr, Sc and Hf. Furthermore, the mylonitisation has helped in substantial concentration of U relative to Th, resulting in low Th/U values of 2 to 0.3, besides decrease in the contents of Rb, Sr and Ce.

3.   The de-silicified or basified mylonite is characterised by Th/U value of < 1, notable Au and Sc contents, suggesting relative enrichment of these elements during chloritisation and biotitisation.

4.   The granite mylonites are marked by metasomatic alterations of biotitisation, sericitisation and chloritisation, all of which brought enrichment of U as well as HREE.

5.   There appears to be positive correlation of U with Fe-Mg trace elements and HREE, and negative correlation with Rb, Sr and LREE.

Schistose rocks (Table 2): These show the following major, minor and trace element patterns.

1.   Compared to the granitoids, the schists are characterised by depletion in silica and Na, and enrichment in U, alumina, Fe^t, MgO, CaO, K_2O, TiO_2, P_2O_5 and LOI, reflected mineralogically in their less content of quartz and sodic plagioclase, and higher contents of biotite, sericite, epidote, sphene and apatite.

2.   In trace element distribution, the schists show mixed patterns, compared to that of the above noted major and minor elemental distribution, which is reflected by their high contents of Rb, Ba, Ni, Co, Cr, V, Ga, Y, U, Sc and Hf, with comparable contents of Au and depletion in Sr, as compared to that of parental biotite granite of Mallammakonda (M-15, Table 1).

3.   The ∑REE content in the schists, as compared to that in biotite granite is 3 or more orders less, with the content of HREE more by the same order (Table 3), reflected by very low values for $(La/Lu)_{cn}$ as well as $(Ce/Yb)_{cn}$.

4.   The chondrite-normalized REE patterns of the schists show gentle slope from light to heavy REE, with positive Eu-anomaly in one in contrast to steep slope from light to heavy REE with no Eu-anomaly of the granites (Fig. 3a).

5.   The schistose rocks resemble the de-silicified granite mylonite in some of the major, minor and trace element distribution patterns, *viz.,* low-silica and ∑REE with positive Eu-anomaly, as well as higher content of alumina, Fe^t, Mg, Au, Ni, Co, Sc, Cr and U. However, the schists, as compared to silica-depleted granite mylonite are marked by higher contents of K and its related trace elements like Rb and Ba as well as CaO, TiO_2 and P_2O_5.

6.   The above noted elemental patterns of the schistose rocks and the granite mylonites, compared together with that of parental biotite granite of Mallammakonda, point to Fe-Mg-Ca-Na-Ti-P metasomatism simultaneous with silica depletion, with their intensity being relatively more in the schists and less in the silica-depleted mylonites. Furthermore, these metasomatic processes appear to have helped the mobilisation and higher concentration of U, besides, Au, Sc, Hf and HREE, which show a sympathetic variation with values of U and U/Th.

From the above geochemical account on the schistose rocks, the following are the *inferences* drawn:

1.   The parental, unaltered or least biotite granite of Mallammakonda, when subjected to dislocation metamorphism and attending K-Fe-Mg-Ca-P-Ti metasomatism, led to the formation of silica-depleted granite mylonites and schistose granites that comprise major amounts of biotite, sericite, chlorite, epidote, sphene and minor apatite.

2.   The above metasomatic changes have helped in the remobilisation of both U and the so called immobile elements like Ti, Zr, Hf, Y and HREE, leading to their relative enrichment in both the silica-depleted and Mg-Fe-enriched mylonites and schists.

Gudarukoppu (G) area
Migmatite (Table 1): Major, minor and trace element, including REE, patterns of migmatite are as follows:

1.   In the field, this rock looks like a migmatite and mineralogy-wise, it is a 2-mica, peraluminous, low-Ca granite with relatively higher content of P_2O_5.

2.   Trace element-wise, it shows depletion in Rb, Sr and Ba as well as in immobile and ferromagnesian trace elements, as compared to the average low-Ca granite (*cf.* Turekian and Wedepohl, 1961).

3.   Its U-content is 2 orders more while Th is less by more or less same order, as compared to the low-Ca granite, leading to low value of 1 for Th/U.

4.   The ∑ REE content (Table 3) is low, around 80 ppm, with moderate enrichment of LREE over HREE, reflected by (La/Lu)cn of 7.6 and (Ce/Yb)cn of 5, with no Eu-anomaly (Fig. 3b).

Phyllites and Schists (Table 2): Major, minor and trace element, including REE, patterns of these rocks are as follows:

1.   These rocks, containing 2-micas, chlorite and quartz as major minerals, are basic to intermediate 52-62 wt. % silica and marked enrichment in Fe^t, K_2O, TiO_2 and P_2O_5.

2.   Trace element-wise, these rocks are characterised by high contents of Ni, Co, Cr, V, Rb, Ba and Ga.

3.   Out of the 4 analysed samples (Table 2), 3 are showing depletion in Ca and Sr, whereas the other is showing enrichment of both these elements.

4.   Of the 2 analysed samples of phyllites, the ∑ REE varies from 133 to 304 ppm (Table 3), with moderate to notable enrichment of LREE over HREE, and both with no Eu-anomaly (Fig. 3b).

5.   In one sample, Au is 48 ppb, whereas both the analysed phyllites are marked by high Sc.

Quartz-apatite rock (as veins; Table 2): This U-mineralised rock occurs mainly as veins and extends up to   ~ 100 m in length and 2-3 in width, within the quartz-biotite cataclasites/schists and is *anomalous* for its apatite content. Its major, minor and trace element, including REE, patterns are as follows:

1.   The quartz-apatite rock is marked by very high content of both CaO and P_2O_5, and very low content of all other radicals, due to the predominance of apatite with lesser quartz in it.

2.   Trace element-wise, this rock is characterised by very high contents of Sr and immobile trace elements like Zr, Y and Res, with Th/U value being < 0.05.

3.   The $\sum$ REE is very high (> 0.2 wt. %) (Table 3), with moderate enrichment of LREE over HREE, reflected in its $(La/Lu)_{cn}$ of 6.5 and $(Ce/Yb)_{cn}$ of 3, with negligible negative Eu-anomaly (Fig. 3b).

Apatite-bearing biotite-quartz cataclasite (Table 2): This rock, containing veins of the above described quartz-apatite rock, appears to be alkali metasomatised granitoid, with the precursor feldspar completely transformed to biotite, albite and a little muscovite. Its major, minor and trace element, including REE, patterns are as follows:

1.   In the major and minor element chemistry, this rock is comparable in many respects with that of a low-Ca, peraluminous granitoid, with the exception being its relatively higher content of P_2O_5 and a little of Fe and Mg.

2.   Trace element-wise, this rock shows mostly depletion in ferromagnesian trace elements as well as Sr, Ba, Rb, Zr and Y, with notable enrichment in U and Ga, resulting in its Th/U < 1 as well as low value for Zr/Hf of ~ 1.5.

3.   The $\sum$ REE content in this rock is 137 ppm (Table 3), with moderate enrichment of LREE over HREE and no Eu-anomaly (Fig. 3b).

From the above geochemical account on the analysed rock types from the Gudarukoppu area, the following are the *inferences* drawn:

1.   Almost all the rock types analysed from this area appear to have been subjected to variable degree of metasomatic activity, *viz.,* alkali metasomatism (mainly K-metasomatism) and P-metasomatism, with the latter of very high degree resulting in quartz-apatite rock (as veins).

2.   The Mallammakonda biotite granite, subjected to a lesser degree of alteration, is marked by depletion in Rb, Ba and Sr, implying probably their migration from it.

3.   The higher concentration of Rb, Ba and Sr in the nearby apatite-bearing quartz-biotite cataclasite suggests that during alkali metasomatism, these elements, due to their characteristic easy mobility, were concentrated in the cataclasite.

4.   The Th/U value in all the analysed rocks from this area, as given above, is much low, at 0.05-1, with the lowest value being in the quartz-apatite cataclasite, In contrast, the high value of Th/U up to 10 in the quartzite (analysis not given) in the area implies that there is not much loss of both Th and U from the quartzite, since these radio-elements are locked in its accessory and refractory minerals of monazite and zircon.

5.   The generally low value for Th/U, culminating with the highest content of U in quartz-apatite (vein) rock, together with its notable amount of secondary U-mineral (*Uranophane*) in it, points out that the labile U of the unaltered biotite granitoid got remobilized and concentrated in the metasomatic rocks like apatite-biotite schist, phyllite and quartz-apatite rock. Thus, the remobilisation and concentration of U in the study area are to a great extent controlled by alkali, especially K, metasomatism.

6.   Apart from the alkali metasomatism, minor amount of Fe-Mg-B metasomatism had also affected the rocks in the area, which is manifested as secondary biotite, chlorite and tourmaline. It is possible that some amount of Mg and Fe for this could have contributed by basic intrusive rocks in the area like amphibolites, since these amphibolites from the nearby Kasturigattu (K) area being of low-Mg amphibolites marked with depletion in Ni, Co, Cr and U, compared to average basalt (chemical data on 'amphibolites' are not given in this paper).

7.   The chondrite-normalized REE patterns of most of the analysed rocks in the G-area (Fig. 3b) show almost no Eu-anomaly, with many rocks showing moderate enrichment of LREE over HREE, whereas the quartz-apatite (vein) rock is marked by very high content of > 0.2% $\sum$ REE as also very high enrichment of LREE over HREE.

8.   The Zr/Hf value, generally considered as not affected by alteration and metamorphism, seems to have been affected by metasomatism in the area, as documented by wide range of its value from 13 to 65.

VI. Controls of U-mineralisation

The following are the controls of U-mineralisation in the Kasturigattu (K) – Gudarukoppu (G) area:

1.   *Structural* in the form of shear zone that covers almost the entire K – G area;

2.   *Petrological* in the form fertile (for U), peraluminous biotite granitoid and its deformed – metamorphic – metasomatic variants in the form of granite cataclasite and mylonite, and schists/phyllites with major mineralogy of quartz, feldspar, biotite, sericite and chlorite, and apatite-rich quartz-apatite (vein) rock;

3.   *Mineralogical alterations* of biotitisation, sericitisation, chloritisation and apatitisation, the last mostly in the Gudarukoppu area;

4.   *Geochemical* in the form of *silicified* and *de-silicified* deformed-metamorphic-metasomatic variants of parental, fertile biotite granite, with the latter more potential for higher concentration of U; and

5.   *Metamorphism* of low- to medium-grade – greenschist to epidote-amphibolite facies – and K-Fe-Mg-P-Ti-B *metasomatism.*
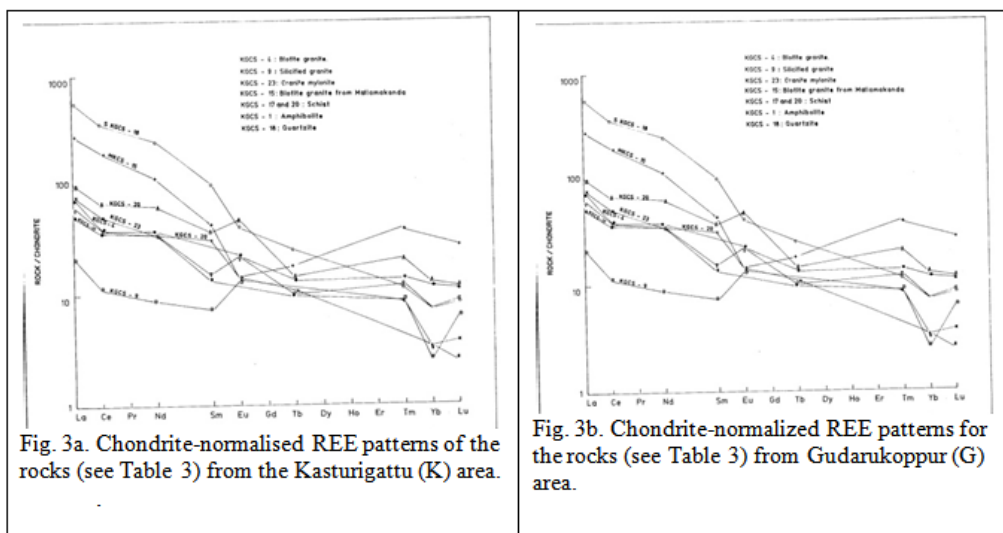
Fig. 3a. Chondrite-normalised REE patterns of the rocks (see Table 3) from the Kasturigattu (K) area.

Fig. 3b. Chondrite-normalized REE patterns for the rocks (see Table 3) from Gudarukoppur (G) area.

VII. Conclusions

Shear zone-hosted U-mineralisation occurs in the Kasturigattu (K) – Gudarukoppu (G) area, forming a part of the Crystalline Complex (CC) in the SE environs of the Cuddapah basin. Of the different rock types in CC, the fertile (for U) biotite granite, forming the basement, and its deformed-metamorphic-metasomatic variants occurring in the form of granite cataclasite and mylonite, and schists (phyllites) with major mineralogy of quartz, feldslpars, biotite, sericite, chlorite, epidote, sphene and apatite as well as quartz-apatite (vein) rock are important from the point of U-mineralisation. Petrography, mineragraphy and whole-rock geochemistry in terms of major, minor and trace, including Rare Earth, elements of these rocks are presented, together with brief accounts of their geological setting, methods adopted and materials used, mineralogical alterations, metamorphic and K-Fe-Mg-P metasomatic aspects. Bearing of these aspects on the 2 types of U-mineralisation in the area, *viz.,* older, high-temperature, syn-magmatic type, manifested as inclusions of *uraninite* in the gangue, and more widespread, important, low-temperature, hydro (epi)-thermal type in the form of *coffinite* and *pitchblende*, present along the weak planes and as vein-lets, in addition to fracture-fillings and encrustations of secondary U-mineral (*uranophane*), is discussed, based on which the controls of U-mineralisation are advanced. Whenever extraction of U in this area is feasible, LREE-rich (up to 0.23 wt. %) apatite will be a high-value by-product.

Acknowledgements

References

[1]. Bidwai, R. and Madhusudan Rao (1988) Radiometric survey in the basement granitoid along the southwestern margin of the Cuddapah basin. Ann. Rep. for the Field Season, 1987-88, Southern Region, AMD, Bangalore (Unpublished).

[2]. Dhana Raju, R. (2009) Cuddapah basin: India's emerging Uranium-Hub. J. Ind. Assoc. Sedimentologists, 28 (2), pp. 15-24.

[3]. Dhana Raju, R.(2009a) Handbook of Geochemistry: Techniques and Applications in Mineral Exploration. Geol. Soc. India, Bangalore, India, 520 p.

[4]. Dhana Raju, R (2009b) Handbook of Mineral Exploration and Ore Petrology: Techniques and Applications. Geol. Soc. India, Bangalore, India, 494 p.

[5]. Dhana Raju, R., Lakshminarayana, Y. and Sudhakar, Ch. (2018) Uranium mineralisation around Mulapalle, SW of Lakkireddipalle, Kadapa district, Andhra Pradesh, Inida and Laboratory-Scale Processing of its Uranium Ore. IOSR-Jour. Applied Geol. Geophysics (IOSR- JAGG, online journal), 6 (5), pp. 86-95.

[6]. Dhana Raju, R., Lakshminarayana, Y. and Sudhakar, Ch. (2018a) Uranium mineralisation around Kasturigattu, SE-margin of the Cuddapah basin, India and Laboratory-scale mineral processing of its uranium ore. IOSR-Jour. Applied Geol. Geophysics (IOSR-JAGG, online journal), 6 (5), pp. 22-29.

[7]. Dhana Raju, R., Lakshminarayana, Y. and Sudhakar, Ch. (2018b) Uranium mineralisation from Gudarukoppu, SE-margin of the Cuddapah basin, A.P., India and Laboratory-scale mineral processing of its Uranium Ore. Intl. Jour. Dev. Res. (IJDR, online journal), 8 (8), pp. 22507-22514.

[8]. Dhana Raju, R., Umameshwar, K., Tripathi, B.K., Rai, A.K., Zakaulla, S., Thirupathi, P.V. and Nanda, L.K. (2002) Structurally-controlled and crystalline rock-hosted uranium mineralization in the southern environs of the Cuddapah basin, Andhra Pradesh, India. Expl. Res.At. Miner. 14, pp. 95-108.

[9]. Dutt, N.V.B.S. (1986) Geology and Mineral Resources of Andhra Pradesh. 3rd Ed., Natural Resources Development Co-operative Society (NRDCS), Hyderabad, 434 p.

[10]. Geological Survey of India (1975) Geological and Mineral Resources of Andhra Pradesh. Misc. Publ. No. 30, Pt. 8,- Andhra Pradesh, pp. 1- 51. Jeyagopal, A.V. and Dhana Raju, R. (1998) Recognition criteria and sedimentology of the dolostone-hosted stratabound uranium mineralization in Vempalle formation, Cuddapah basin, Andhra Pradesh, India. *In*: (Ed. R.N. Tiwari) Recent Researches in Sedimentary Basins, Proceedings of the National Symposium, Indian Petroleum Publishers, Dehra Dun, pp. 172-179.

[11]. Jeyagopal, A.V., Kumar, P. and Sinha, R.M. (1996) Uranium mineralisation in the Palnadu sub-basin, Cuddapah basin, Andhra Pradesh, India. Curr. Sci. 71, pp.957-959.

[12]. Kurien, T.K. (1980) Geology and Mineral Resources of Andhra Pradesh. Bulle. Geol. Surv. India, Series A, Economic Geology, No. 42, 242 p.

[13]. Leelanandam, C. (1991) The Kandra Vocanics in Andhra Pradesh: Possible Ophiolite? Curr. Sci. 59 (16), pp. 785-788.

[14]. Nagaraja Rao, B.K., Rajurkar, S.T., Ramalingaswamy, G. And Ravindra Babu, B. (1987) Stratigraphy, structure and evolution of the Cuddapah basin. Purana basins of the Peninsular India. Geol. Soc. India Mem. 6, pp. 33-86.

[15]. Rai, A.K., Chopra, R. and Veerabhaskar, D. (1992) Rep. for Field Season, 1992-93. Southern Region, AMD, Bangalore (Unpublished).

[16]. Rai, A.K., Sharma, S.K., Umamaheswar, K., Nagabhushana, J.C. and Vasudeva Rao, M. (1995) Uranium mineralization in the eastern margin of Cuddapah basin. Abstract vol., Geol. Soc. India Ann. Conv. and Seminar on 'Cuddapah basin', Thirupati, Sept. 9-12.

[17]. Satyanarayana, K. (1986) Geochemistry of amphibolites and associated rocks in parts of the Nellore-Gudur pegmatite belt, Andhra Pradesh, India. Ph.D. thesis in Geology, Faculty of Science, Osmania University, Hyderabad, India, 286 p.

[18]. Sinha, R.M., Shrivastava, S.K., Sarma, G.V.G. and Parthasarathy, T.N. (1995) Geological favourability for unconformity related uranium deposits in the northern parts of the Cuddapah Basin: Evidence from Lambapur uranium occurrences, Andhra Pradesh, India. Expl. Res. At. Miner. 8, pp. 111-126.

[19]. Sundaram, S.M., Sinha, P.A., Ravindra Babu, B. And Muthu, V.T. (1989) Uranium mineralisation in Vempalli Dolomite and Pulivendla conglomerate/quartzite of Cuddapah basin, A.P. Indian Minerals, 43 (2), pp. 98-103.

[20]. Sudhakar, Ch. (1996) Geochemistry of the crystalline rocks around Rayachoti, Cuddapah district and Kasturigattu, Nellore district, Andhra Pradesh, India. Ph.D. thesis in Geology, Faculty of Science, Bangalore University, Bangalore, India, 181 p.

[21]. Thimmaiah, M., Ramachar, T.M., Veerabhaskar, D. and Jayaram, K.M.V. (1986) The uraniferous biotite-sericite schist of Kasturigattu hillock, north-east of Somasila, Nellore district, Andhra Pradesh. Curr. Sci. 55, p. 350.

[22]. Thirupathi, P.V., Sudhakar, Ch., Krishna, K.V.G. and Dhana Raju, R. (1996). Petrology and Geochemistry of the Proterozoic A-type Granite of Kanigiri, Prakasam district, Andhra Pradesh: Implications for rare metal mineralisation. Expl. Res. At. Miner. (EARFAM) 9, 61-72.

[23]. Turekian, K.K. and Wedepohl, K.H. (1961). Distribution of Elements in some major units of the Earth's crust. Geol. Soc. Amer. Bulle., 72, pp. 175-192.

[24]. Umamaheswar, K., Sharma, U.P., Zakaulla, S., Basu, H., Thomas, A.M. and Ali, M.A. (2001) Occurrence of gold in association with uranium in Gulcheru quartzite of Cuddapah basin, Gandi – Rachakuntapalle area, Cuddapah district, Andhra Pradesh. Curr. Sci. 81 (7), pp. 754-756.

[25]. Vasudeva Rao, M., Nagabhushana, J.C. and Jeyagopal, A.V. (1989) Uranium mineralization in the Middle Proterozoic carbonate rock of the Cuddapah Suprgroup, Southern Peninsular India. Expl. Res. At. Miner. 2, pp. 29-38.

[26]. Veerabhaskar, D., Sarkar, M., Thimmaiah, M., Sharma, M. and Dhana Raju, R. (1991) Uranium mineralization at Kasturigattu, Nellore district, Andhra Pradesh, India: An example of shear-controlled, syngenetic- remobi-lizedtype in Proterozoic Granitic and low-grade metamorphic rocks. Expl. Res. At. Miner. 4, pp. 27-37.